A&A 455, 679–684 (2006)
DOI: 10.1051/0004-6361:20065102

Astronomy & Astrophysics

On the relevance of Compton scattering for the soft X-ray spectra of hot DA white dwarfs

V. Suleimanov[1,2,5], J. Madej[3], J. J. Drake[4], T. Rauch[1], and K. Werner[1]

[1] Institut für Astronomie und Astrophysik, Universität Tübingen, Sand 1, 72076 Tübingen, Germany
e-mail: suleimanov@astro.uni-tuebingen.de
[2] Kazan State University, Kremlevskaja str., 18, Kazan 420008, Russia
[3] Warsaw University Observatory, Al. Ujazdowskie 4, 00-478 Warsaw, Poland
[4] Smithsonian Astrophysical Observatory, MS-3, 60 Garden Street, Cambridge, MA 02138, USA
[5] Kazan Branch of Isaac Newton Institute, Santiago, Chile

Received 27 February 2006 / Accepted 7 May 2006

ABSTRACT

Aims. We re-examine the effects of Compton scattering on the emergent spectra of hot DA white dwarfs in the soft X-ray range. Earlier studies have implied that sensitive X-ray observations at wavelengths $\lambda < 50$ Å might be capable of probing the flux deficits predicted by the redistribution of electron-scattered X-ray photons toward longer wavelengths.

Methods. We adopt two independent numerical approaches to the inclusion of Compton scattering in the computation of pure hydrogen atmospheres in hydrostatic equilibrium. One employs the Kompaneets diffusion approximation formalism, while the other uses the cross-sections and redistribution functions of Guilbert. Models and emergent spectra are computed for stellar parameters representative of HZ 43 and Sirius B, and for models with an effective temperature $T_{\rm eff} = 100\,000$ K.

Results. The differences between emergent spectra computed for Compton and Thomson scattering cases are completely negligible in the case of both HZ 43 and Sirius B models, and are also negligible for all practical purposes for models with temperatures as high as $T_{\rm eff} = 100\,000$ K. Models of the soft X-ray flux from these stars are instead dominated by uncertainties in their fundamental parameters.

Key words. radiative transfer – scattering – methods: numerical – stars: white dwarfs – stars: atmospheres – X-rays: stars

1. Introduction

The scattering of radiation by free electrons is one of the dominant sources of continuous opacity in the atmospheres of hot white dwarfs. Most model atmosphere calculations adopt the classical Thomson isotropic scattering approach, whereby only the direction of photon propagation changes as the result of a scattering event. More rigorously, finite electron mass instead implies that both momentum and energy exchange should actually occur.

The effects of Compton scattering on white dwarf model atmospheres was first investigated in detail by Madej (1994), who found that pure hydrogen models with temperatures of 10^5 K show a significant depression of the X-ray continuum for wavelengths <50 Å. Effects for models containing significant amounts of helium, or helium and heavier elements, were found to be much smaller or negligible, in keeping with expectations based on the relative importance of electron scattering as an opacity source as opposed to photoelectric absorption.

In a later paper, Madej (1998) computed the effects of Compton scattering for a model corresponding to the parameters of the DA white dwarf HZ 43. Differences between Compton and Thomson scattering model spectra were apparent for $\lambda < 50$ Å, and grew to orders of magnitude by 40 Å. While current X-ray instrumentation is not sufficiently sensitive to study the spectra of even the brightest DA white dwarfs in any detail at wavelengths $\lambda < 50$ Å, the spectral differences implied by the more rigorous Compton redistribution formalism will be of interest to more sensitive future missions. Moreover, the *Chandra* Low Energy Transmission Grating Spectrometer (LETG+HRC-S) effective area calibration is based on observed spectra of HZ 43 and Sirius B at wavelengths $\lambda > 60$ Å (Pease et al. 2003). It is therefore of current topical interest to re-examine the influence of Compton scattering for these stars and determine whether any significant differences might be discernible between Thomson and Compton scattering in the LETGS bandpass.

In this paper, we perform two independent and rigorous tests of the influence of Compton scattering on the emergent spectra of hot DA white dwarfs. Our methods of calculation are outlined in Sect. 2, while results and conclusions are briefly discussed in Sects. 3–5.

2. Computational methods

In both our numerical approaches, outlined below, we computed model atmospheres of hot white dwarfs subject to the constraints of hydrostatic and radiative equilibrium assuming planar geometry using standard methods (e.g. Mihalas 1978). The equation of state of an ideal gas used assumes local thermodynamic equilibrium (LTE), and therefore did not include terms describing the local radiation field.

The model atmosphere structure for a hot WD is described by the hydrostatic equilibrium equation,

$$\frac{{\rm d}P_{\rm g}}{{\rm d}m} = \frac{GM_{\rm wd}}{R^2_{\rm wd}} - 4\pi \int_0^\infty H_\nu \frac{k_\nu + \sigma_\nu}{c} {\rm d}\nu, \quad (1)$$

where k_ν is opacity per unit mass due to free-free, bound-free and bound-bound transitions, σ_ν is the electron (Compton) opacity, H_ν is Eddington flux, $P_{\rm g}$ is the gas pressure, and m is the column density

$$\mathrm{d}m = -\rho\,\mathrm{d}z. \quad (2)$$

Variable ρ denotes the gas density and z is the vertical distance. As is obvious from Eq. (1), the structure of the atmosphere is coupled to the radiation field and the structure and radiative transfer equations need to be solved simultaneously under the constraint of radiative equilibrium.

In the Thomson approximation, in which no energy or momentum between photons and electrons is exchanged, $\sigma_\nu = \sigma_{\rm e}$, where $\sigma_{\rm e}$ is the classical Thomson opacity.

2.1. Method 1

In our first approach, Compton scattering is taken into account in the radiation transfer equation using the Kompaneets operator (Kompaneets 1957; Zavlin & Shibanov 1991; Grebenev & Sunyaev 2002):

$$\frac{\partial^2 f_\nu J_\nu}{\partial \tau_\nu^2} = \frac{k_\nu}{k_\nu+\sigma_{\rm e}}(J_\nu - B_\nu) - \frac{\sigma_{\rm e}}{k_\nu+\sigma_{\rm e}}\frac{kT}{m_{\rm e}c^2} \times x\frac{\partial}{\partial x}\left(x\frac{\partial J_\nu}{\partial x} - 3J_\nu + \frac{T_{\rm eff}}{T}xJ_\nu\left(1+\frac{CJ_\nu}{x^3}\right)\right), \quad (3)$$

where $x = h\nu/kT_{\rm eff}$ is the dimensionless frequency, $f_\nu(\tau_\nu) \approx 1/3$ is the variable Eddington factor, J_ν is the mean intensity of radiation, B_ν is the black body (Planck) intensity, T is the local electron temperature, $T_{\rm eff}$ is the effective temperature of WD, and $C = c^2h^2/2(kT_{\rm eff})^3$. The optical depth τ_ν is defined as

$$\mathrm{d}\tau_\nu = (k_\nu + \sigma_{\rm e})\,\mathrm{d}m. \quad (4)$$

These equations have to be completed by the energy balance equation

$$\int_0^\infty k_\nu (J_\nu - B_\nu)\,\mathrm{d}\nu - \sigma_{\rm e}\frac{kT}{m_{\rm e}c^2} \times\left(4\int_0^\infty J_\nu\,\mathrm{d}\nu - \frac{T_{\rm eff}}{T}\int_0^\infty xJ_\nu\left(1+\frac{CJ_\nu}{x^3}\right)\mathrm{d}\nu\right) = 0, \quad (5)$$

the ideal gas law

$$P_{\rm g} = N_{\rm tot}kT, \quad (6)$$

where $N_{\rm tot}$ is the number density of all particles, and also by the particle and charge conservation equations. We assume local thermodynamical equilibrium (LTE) in our calculations, so the number densities of all ionisation and excitation states of all elements have been calculated using Boltzmann and Saha equations.

For solving the above equations and computing the model atmosphere we used a version of the computer code ATLAS (Kurucz 1970, 1993), modified to deal with high temperatures; see Ibragimov et al. (2003) and Swartz et al. (2002) for further details. This code was also modified to account for Compton scattering.

The scheme of calculations is as follows. First of all, the input parameters of the WD are defined: the effective temperature $T_{\rm eff}$ and surface gravity $g = GM_{\rm wd}/R^2_{\rm wd}$. Then a starting model using a grey temperature distribution is calculated. The calculations are performed with a set of 98 depth points $m_{\rm i}$ distributed logarithmically in equal steps from $m \approx 10^{-6}$ g cm^{-2} to $m_{\rm max}$. The appropriate value of $m_{\rm max}$ is found from the condition $\sqrt{\tau_{\nu,{\rm b-f,f-f}}(m_{\rm max})\tau_\nu(m_{\rm max})} > 1$ at all frequencies. Satisfying this equation is necessary for the inner boundary condition of the radiation transfer.

For the starting model, all number densities and opacities at all depth points and all frequencies (we use 300 logarithmically equidistant frequency points) are calculated. The radiation transfer Eq. (3) is non-linear and is solved iteratively by the Feautrier method (Mihalas 1978, see also Zavlin & Shibanov 1991; Pavlov et al. 1991; Grebenev & Sunyaev 2002). We use the last term of the Eq. (3) in the form $xJ^i_\nu(1 + CJ^{i-1}_\nu/x^3)$, where J^{i-1}_ν is the mean intensity from the previous iteration. During the first iteration we take $J^{i-1}_\nu = 0$. Between iterations we calculate the variable Eddington factors f_ν and h_ν, using the formal solution of the radiation transfer equation in three angles at each frequency. Usually 2–3 iterations are sufficient to achieve convergence.

We used the usual condition at the outer boundary

$$\frac{\partial J_\nu}{\partial \tau_\nu} = h_\nu J_\nu, \quad (7)$$

where $h_\nu \approx 1/2$ is surface variable Eddington factor. The inner boundary condition is

$$\frac{\partial J_\nu}{\partial \tau_\nu} = \frac{\partial B_\nu}{\partial \tau_\nu}. \quad (8)$$

The outer boundary condition is found from the lack of incoming radiation at the WD surface, and the inner boundary condition is obtained from the diffusion approximation $J_\nu \approx B_\nu$ and $H_\nu \approx 1/3 \times \partial B_\nu/\partial\tau_\nu$.

The boundary conditions along the frequency axis are

$$J_\nu = B_\nu \quad (9)$$

at the lower frequency boundary ($\nu_{\rm min} = 10^{12}$ Hz, $h\nu_{\rm min} \ll kT_{\rm eff}$) and

$$x\frac{\partial J_\nu}{\partial x} - 3J_\nu + \frac{T_{\rm eff}}{T}xJ_\nu\left(1+\frac{CJ_\nu}{x^3}\right) = 0 \quad (10)$$

at the higher frequency boundary ($\nu_{\rm max} \approx 3\times10^{17}$ Hz, $h\nu_{\rm max} \gg kT_{\rm eff}$). Condition (9) means that at the lowest energies the true opacity dominates the scattering $k_\nu \gg \sigma_{\rm e}$, and therefore $J_\nu \approx B_\nu$. Condition (10) means that there is no photon flux along frequency axis at the highest energy.

The solution of the radiative transfer Eq. (3) was checked for the energy balance Eq. (5) together with the surface flux condition

$$4\pi\int_0^\infty H_\nu(m=0)\mathrm{d}\nu = \sigma T^4_{\rm eff} = 4\pi H_0. \quad (11)$$

The relative flux error as a function of depth,

$$\varepsilon_{\rm H}(m) = 1 - \frac{H_0}{\int_0^\infty H_\nu(m)\mathrm{d}\nu}, \quad (12)$$

was calculated, where $H_\nu(m)$ is radiation flux at given depth. This latter quantity was found from the first moment of the radiation transfer equation:

$$\frac{\partial f_\nu J_\nu}{\partial \tau_\nu} = H_\nu. \quad (13)$$

Temperature corrections were then evaluated using three different procedures. The first is the integral Λ-iteration method, modified for Compton scattering, based on the energy balance Eq. (5). It is valid in the upper atmospheric layers. The second

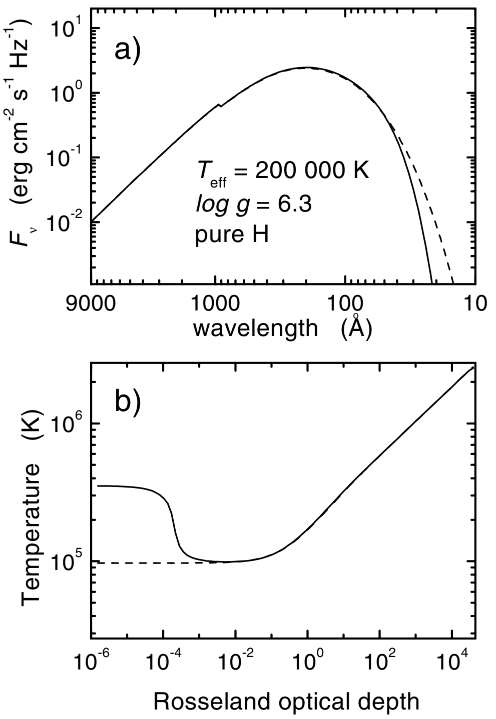

Fig. 1. Spectra **a)** and temperature structures **b)** of a hot DA white dwarf model atmosphere with $T_{\rm eff}$ = 200 000 K and log g = 6.3 with (solid line) and without (dashed line) Compton scattering taken into account.

one is the Avrett-Krook flux correction, which uses the relative flux error, and is valid in the deep layers. And the third one is the surface correction, which is based on the emergent flux error. See Kurucz (1970) for a detailed description of the methods.

The iteration procedure is repeated until the relative flux error is smaller than 1%, and the relative flux derivative error is smaller than 0.01%. As a result of these calculations, we obtain the self-consistent WD model atmosphere together with the emergent spectrum of radiation.

Our method of calculation was tested on a model of bursting neutron star atmospheres (Pavlov et al. 1991; Madej 1991), and a model DA white dwarf atmosphere with $T_{\rm eff} = 2 \times 10^5$ K, log g = 6.3 (Madej 1994). Agreement with the earlier calculations is extremely good. We show the emergent spectrum from the latter calculation in Fig. 1.

2.2. Method 2

Our second approach adopts the equation of transfer for absorption and scattering presented by Sampson (1959) and Pomraning (1973, see Eq. (2.167)). The equation of transfer can be expressed in the form

$$\frac{\partial^2 f_\nu J_\nu}{\partial \tau_\nu^2} = \frac{k_\nu}{k_\nu+\sigma_\nu}(J_\nu - B_\nu) + \frac{\sigma_\nu}{k_\nu+\sigma_\nu} J_\nu \int_0^\infty \Phi(\nu,\nu')\left(1+\frac{c^2}{2h\nu'^3}J_{\nu'}\right)\mathrm{d}\nu' - \frac{\sigma_\nu}{k_\nu+\sigma_\nu}\left(1+\frac{c^2}{2h\nu^3}J_\nu\right) \times \int_0^\infty \Phi(\nu,\nu')J_{\nu'}\left(\frac{\nu}{\nu'}\right)^3 \exp\left[-\frac{h(\nu-\nu')}{kT}\right]\mathrm{d}\nu'. \tag{14}$$

This transfer equation is written on the monochromatic optical depth scale $\mathrm{d}\tau_\nu = -(k_\nu + \sigma_\nu)\rho\,\mathrm{d}z$. The variable J_ν denotes the energy-dependent mean intensity of radiation. The function $\Phi(\nu,\nu')$ denotes the zeroth angular moment of the angle-dependent differential cross-section, normalized to unity (see below).

Transformation of the equation of transfer by Pomraning (1973) to Eq. (14) and the definition of required angular approximations for Compton scattering in a stellar atmosphere was outlined by Madej (1991, 1994) and Madej et al. (2004).

Our equations and theoretical models of Method 2 use detailed differential cross-sections for Compton scattering, $\sigma(\nu \rightarrow \nu', \boldsymbol{n}\cdot\boldsymbol{n}')$, which were taken from Guilbert (1981). Cross-sections correspond to scattering in a gas of free electrons with relativistic thermal velocities, and they are also completely valid at low temperatures. Differential cross-sections were then integrated numerically to obtain large grids of Compton scattering opacity coefficients σ_ν

$$\sigma_\nu = \oint_{\omega'} \frac{\mathrm{d}\omega'}{4\pi}\int_0^\infty \mathrm{d}\nu'\,\sigma(\nu\rightarrow\nu',\boldsymbol{n}\cdot\boldsymbol{n}'), \tag{15}$$

and grids of angle-averaged Compton scattering redistribution functions $\Phi(\nu,\nu')$

$$\Phi(\nu,\nu') = \frac{1}{\sigma_\nu}\oint_{\omega'}\frac{\mathrm{d}\omega'}{4\pi}\,\sigma(\nu\rightarrow\nu',\boldsymbol{n}\cdot\boldsymbol{n}'). \tag{16}$$

The scattering frequency redistribution function was introduced by Pomraning (1973) – see Eq. (7.95) of his book – and it represents the normalized probability density of scattering from a given frequency ν to the outgoing frequency ν'.

Note that Eq. (14) also includes stimulated scattering terms, $1 + (c^2/2h\nu^3)\,J_\nu$, which ensure the physically correct description of Compton scattering. The actual equations and calculations used here strongly differ from those in Madej (1998). The physics of Compton scattering used here is also fundamentally different to Method 1. Note, that the latter method and that of Madej (1998) employ the well-known Kompaneets diffusion approximation to Compton scattering kernels. The apparent difference between Methods 1 and 2 is that they use either the differential Kompaneets kernel (Method 1) or kernels given by integrals over the detailed Compton scattering profiles (Method 2).

The equation of radiative equilibrium (the energy balance equation) requires that

$$\int_0^\infty H_\nu\,\mathrm{d}\nu = \frac{\sigma_R T_{\rm eff}^4}{4\pi}. \tag{17}$$

The above condition is fulfilled in a hot stellar atmosphere, where energy transport by convective motions can be neglected.

Computing derivatives of both sides of Eq. (17) and using the equation of transfer, Eq. (14), one can obtain the alternative energy balance equation

$$\int_0^\infty k_\nu(J_\nu - B_\nu)\,\mathrm{d}\nu + \int_0^\infty \sigma_\nu J_\nu \mathrm{d}\nu \int_0^\infty \Phi(\nu,\nu')\left(1+\frac{c^2}{2h\nu'^3}J_{\nu'}\right)\mathrm{d}\nu' - \int_0^\infty \sigma_\nu\left(1+\frac{c^2}{2h\nu^3}J_\nu\right)\mathrm{d}\nu \int_0^\infty J_{\nu'}\,\Phi(\nu,\nu')\left(\frac{\nu}{\nu'}\right)^3 \exp\left[-\frac{h(\nu-\nu')}{kT}\right]\mathrm{d}\nu' = 0, \tag{18}$$

which can be compared with its analog, Eq. (5) of Method 1.

The computer code ATM21 used for the model calculations was described in detail in Madej & Różańska (2000) and Madej et al. (2004). The structure of the code is based on the partial linearization scheme by Mihalas (1978), in which corrections of temperature ΔT and the function $\Delta\Phi$ are built into the equation of transfer. The high numerical accuracy and very good convergence properties of the ATM21 code are vital for the present paper, and allowed us to compute accurate spectra for atmospheric parameters appropriate for the white dwarfs HZ 43 and Sirius B using Method 2, outlined above. These calculations supersede less accurate X-ray spectra of HZ 43 which were presented in the earlier paper (Madej 1998).

For the present research, the ATM21 code included numerous bound-free LTE opacities of neutral hydrogen and free-free opacity of ionized hydrogen, which always remains in LTE. No hydrogen lines were included in the actual computations. In each temperature iteration the code solves the equation of hydrostatic equilibrium to obtain stratifications of gas pressure P_g and density ρ in the model atmosphere. After that the ATM21 code solves the set of coupled equations of radiative transfer with implicit temperature corrections and finds the stratification of ΔT in the model atmosphere. The equation of radiative transfer was solved using the Feautrier method and the technique of variable Eddington factors (Mihalas 1978). Boundary conditions along the τ_ν axis were the same as in Method 1. Explicit expressions for the temperature corrections, ΔT, can be found, e.g., in Madej et al. (2004).

3. Computations and results

Using our two independent methods, we investigated the effects of Compton scattering on the emergent spectra of three pure H white dwarf models. These were: models appropriate for the well-known DA white dwarfs Sirius B (assuming $T_{\rm eff}$ = 24 700 K, log g = 8.6) and HZ 43 ($T_{\rm eff}$ = 50 000 K, log g = 8.0), together with a significantly hotter model with $T_{\rm eff} = 1 \times 10^5$ K and log g = 6 and 8. These models cover the effective temperature range relevant to pure H DA atmospheres and specifically address the question of whether Compton scattering might be relevant to the X-ray bright DA white dwarfs Sirius B and HZ 43 that are central to the low-energy calibration of *Chandra* (Pease et al. 2003).

The results of our calculations from both methods are presented in Figs. 2–5. In Fig. 2a the spectra of the model atmosphere for the DA white dwarf HZ 43 ($T_{\rm eff}$ = 50 000 K, log g = 8.0) computed using Method 1 with (solid line) and without (dashed line) Compton effects are shown. We also calculated a non-LTE model atmosphere for HZ 43 using the Tübingen Model Atmosphere Package (TMAP) (Werner et al. 2003) and computed the radiation transfer Eq. (3) with Compton scattering using this non-LTE model atmosphere structure. The corresponding spectra are shown in Fig. 2a by the dotted line and by open circles.

Calculations using Method 2 in LTE are illustrated in Fig. 3. The differences between Compton and Thomson models in these calculations are very similar to the differences found in Method 1 in Fig. 2a, and are significant only at wavelengths <25 Å. The flux in the models with Compton scattering (Method 1) is smaller than the flux in the model without Compton scattering by 0.5% at 50 Å, 1.3% at 40 Å, 7% at 30 Å, and 40% at 20 Å. Similarly, model computations performed with Method 2 yield the following differences for HZ 43: 0.5% at 50 Å, 1.4 % at 40 Å, 5% at 30 Å, and 56% at 20 Å.

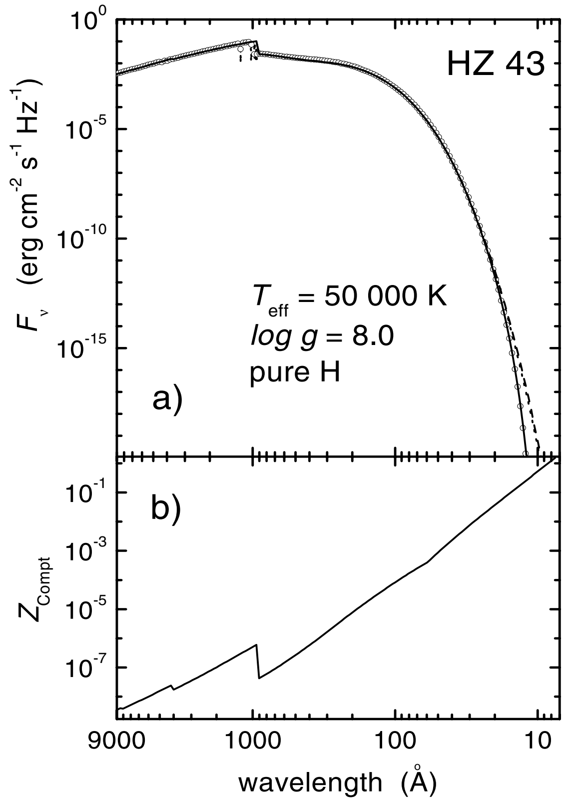

Fig. 2. Spectra **a)** of the DA white dwarf HZ 43 model atmosphere with (solid line) and without (dashed line) Compton scattering using Method 1. Also shown are the spectra of the non-LTE model atmosphere (dotted line) and the spectra of non-LTE model atmosphere with Compton scattering (open circles). Run **b)** of Comptonisation parameter $Z_{\rm Compt}$ with wavelength (see Eq. (19)).

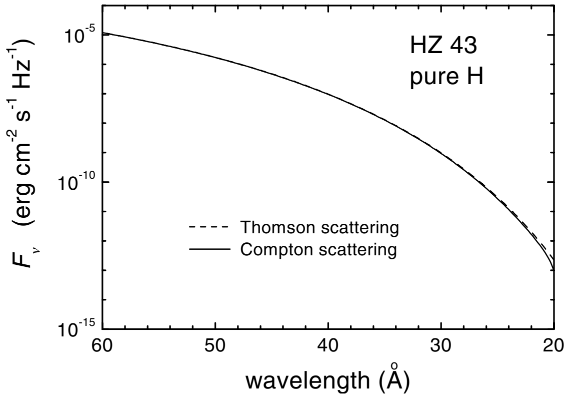

Fig. 3. Emergent X-ray spectra for a pure hydrogen model atmosphere appropriate for the parameters of HZ 43 computed for classical Thomson scattering (dashed) and Compton scattering (solid) using Method 2 (the method of Madej et al. 2004).

These results can be understood more clearly if we consider the Comptonisation parameter $Z_{\rm Compt}$:

$$Z_{\rm Compt} = \frac{h\nu}{m_e c^2} \max\left((\tau_e^*)^2, \tau_e^*\right), \tag{19}$$

where $h\nu/m_e c^2$ is the relative photon energy lost during one scattering event off a cool electron, $\max((\tau_e^*)^2, \tau_e^*)$ is the number of scattering events the photon undergoes before escaping, τ_e^* is the Thomson optical depth, corresponding to the depth where escaping photons of a given frequency are created. The

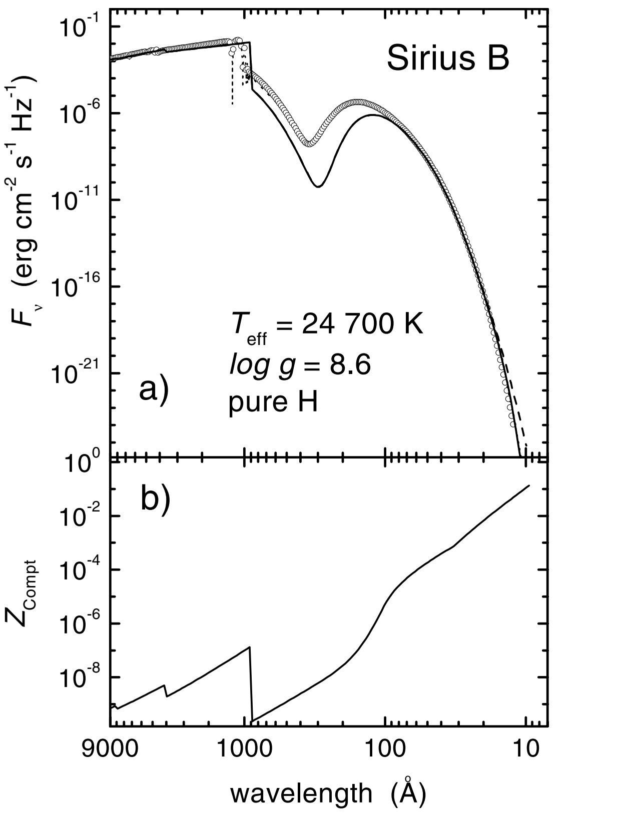

Fig. 4. The same as Fig. 2 but here for the DA white dwarf Sirius B LTE model atmosphere. The dotted line lies everywhere under the open circles (except for hydrogen lines).

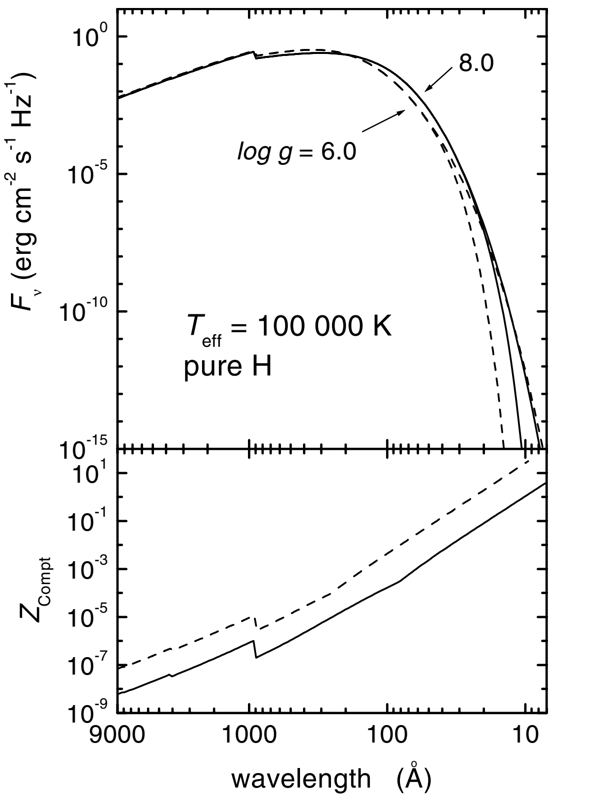

Fig. 5. Spectra **a)** of the DA white dwarf $T_{\rm eff}$ = 100 000 K model atmospheres with and without Compton scattering. Solid lines correspond to model with log g = 8.0, and dashed lines correspond to model with log g = 6.0. Softer high energy tails correspond to models with Compton effect. Run **b)** of Comptonisation parameter $Z_{\rm Compt}$ with wavelength.

Comptonisation parameter is, then, a representation of the influence of Compton down-scattering on the emergent spectrum: significant Compton effects are expected if the Comptonisation parameter approaches unity (Rybicki & Lightman 1979). In Fig. 2b the dependence of $Z_{\rm Compt}$ on the wavelength is shown. It is clear that the Comptonisation parameter is very small down to 25 Å, and this is indeed reflected in the emergent spectrum.

Similar results were obtained for the DA white dwarf Sirius B (assuming $T_{\rm eff}$ = 24 700 K, log g = 8.6). The corresponding spectra and the Comptonisation parameter are shown in Fig. 4. The effective temperature of this star is smaller, and the surface gravity is larger, and consequently Compton scattering is even less significant than for HZ 43. We also calculated a non-LTE model atmosphere for Sirius B using the TMAP and computed the radiation transfer Eq. (3) with Compton scattering using this non-LTE model atmosphere structure, as for HZ 43. The corresponding spectra are shown in Fig. 4a by the dotted line and by open circles. Compton scattering changes only very slightly the emergent spectrum at wavelengths below 20 Å.

In Fig. 5 we present the spectra of the hot DA white dwarf model atmospheres ($T_{\rm eff}$ = 100 000 K, log g = 6 and 8) with and without Compton scattering. It is obvious that Compton effects are more significant for these hot DA models (especially with low surface gravity) than for Sirius B and HZ 43, but visible effects still do not occur for wavelengths >50 Å. Of course, log g = 6 is not such a realistic value for white dwarfs, but we calculate this model to demonstrate the dependence of the Compton effect on the surface gravity.

4. Discussion

The differences we find here between emergent spectra computed using Thomson and Compton scattering are essentially negligible for practical purposes. Such differences are in fact much smaller than the predicted spectral uncertainties resulting from uncertainties in the current knowledge of the fundamental parameters of DA white dwarfs – even the best known examples such as HZ 43 and Sirius B. The spectrum in this Wien tail region is especially sensitive to uncertainties in the effective temperature.

Comparison of the calculations presented here using both Methods 1 and 2 with the earlier work of Madej (1998) do, however, reveal some significant differences. For HZ 43, Fig. 3 of Madej (1998) suggests a large X-ray flux deficit due to Compton scattering of photons to longer wavelengths, with a precipitous decline in emergent flux at ~40 Å. However, our Figs. 2 and 3 illustrate much smaller effects.

A careful examination of the Madej (1998) computer code performed by one of us (JM) has shown that the earlier code (which used Kompaneets scattering terms) could strongly exaggerate effects of Compton scattering in cases when they were of only marginal significance. This is the case for the X-ray spectrum of HZ 43. The effect was caused by an approximation adopted in the solution of the transfer equation that was quite valid for the study of X-ray burst sources, for which the code was primarily developed, but which became marginally inaccurate for the case of hot DA white dwarf atmospheres. This problem has been solved by the very stable algorithm of the new code (see Method 2), described in Madej & Rózańska (2000).

One should note that the differences between this work and that of Madej (1998) are not related to the numerical approaches adopted for Compton scattering. Both the Kompaneets diffusion approximation (Method 1) and the Compton scattering terms of the integral form (Method 2) satisfactorily describe effects of Compton scattering in X-ray spectra of hot white dwarf stars. The results of the work presented here using both methods supersede those of Madej (1998).

At the higher effective temperatures represented by the $T_{\rm eff} = 100\,000$ K models, the emergent spectra for Thomson and Compton scattering begin to diverge at ∼50 Å for the $\log g = 6$ model, and the effects are much larger toward shorter wavelengths than for the higher gravity $\log g = 8$ case. It is of course questionable as to whether any white dwarfs with pure H atmospheres exist with such high effective temperatures, since in hotter stars radiative levitation tends to enrich the atmosphere with metals. In atmospheres with significant metal abundances the electron scattering opacity is insignificant compared with that due to metals, and Compton redistribution effects are rendered irrelevant.

Our calculations show that even in the hottest pure H atmospheres it is highly unlikely that future X-ray observations will be sufficiently sensitive to discern the Compton redistribution effects. Again, uncertainties in model parameters such as effective temperature and surface gravity, and abundances of He and trace elements, together with uncertainties in parameters entering into the modeling calculations themselves will dominate. Even for models normalised to the same flux at UV wavelengths a 1% error in $T_{\rm eff}$ will induce a 20% flux error at 75 Å.

5. Conclusions

New calculations using two independent, rigorous numerical methods confirm that the effects of Compton energy redistribution in photon-electron scattering events are completely negligible for the interpretation of X-ray spectra of DA white dwarfs such as Sirius B and HZ 43. Differences between emergent spectra of Compton and Thomson cases are in fact much smaller than the predicted spectral uncertainties resulting from uncertainties in the current knowledge of the fundamental parameters of stars such as HZ 43. We have found that differences between Compton effects predicted here for HZ 43 and the calculations of Madej (1998) are caused by approximations used in the solution of the transfer equation in the former work; the results presented here supersede the earlier ones. We conclude that current non-LTE model atmosphere spectra of hot DA white dwarfs neglecting Compton scattering can be safely used for the calibration low energy detectors of X-ray observatories for the foreseeable future.

Acknowledgements. V.S. thanks DFG for financial support (grant We 1312/35-1) and Russian FBR (grant 05-02-17744) for partial support of this investigation. J.M. acknowledges support by the Polish Committee for Scientific Research grant No. 1 P03D 001 26. J.J.D. was supported by NASA contract NAS8-39073 to the *Chandra X-ray Center* during the course of this research. T.R. is supported by DLR (grant 50 OR 0201).

References

Grebenev, S. A., & Sunyaev, R. A. 2002, Astron. Lett., 28, 150
Guilbert, P. W. 1981, MNRAS, 197, 451
Ibragimov, A. A., Suleimanov, V. F., Vikhlinin, A., & Sakhibullin, N. A. 2003, Astron. Rep., 47, 186
Kompaneets, A. S. 1957, Sov. Phys. JETP, 4, 730
Kurucz, R. 1993, Atomic data for opacity calculations, Kurucz CD-ROMs, Cambridge, Mass.: Smithsonian Astrophysical Observatory, 1
Kurucz, R. L. 1970, SAO Special Rep., 309
Madej, J. 1991, ApJ, 376, 161
Madej, J. 1994, A&A, 286, 515
Madej, J. 1998, A&A, 340, 617
Madej, J., & Rózańska, A. 2000, A&A, 363, 1055
Madej, J., Joss, P. C., & Różańska, A. 2004, ApJ, 602, 904
Mihalas, D. 1978, Stellar atmospheres, 2nd edition (San Francisco: W. H. Freeman and Co.)
Pavlov, G. G., Shibanov, I. A., & Zavlin, V. E. 1991, MNRAS, 253, 193
Pease, D. O., Drake, J. J., Kashyap, V. L., et al. 2003, in X-Ray and Gamma-Ray Telescopes and Instruments for Astronomy, ed. J. E. Trümper, & H. D. Tananbaum, Proc. SPIE, 4851, 157
Pomraning, G. C. 1973, The equations of radiation hydrodynamics (International Series of Monographs in Natural Philosophy, Oxford: Pergamon Press)
Rybicki, G. B., & Lightman, A. P. 1979, Radiative processes in astrophysics (New York: Wiley-Interscience)
Sampson, D. H. 1959, ApJ, 129, 734
Swartz, D. A., Ghosh, K. K., Suleimanov, V., Tennant, A. F., & Wu, K. 2002, ApJ, 574, 382
Werner, K., Deetjen, J. L., Dreizler, S., Nagel, T., Rauch, T., & Schuh, S. L. 2003, in Stellar Atmosphere Modeling, ASP Conf. Ser., 288, 31
Zavlin, V. E., & Shibanov, Y. A. 1991, Sov. Astron., 35, 499